Applied Magnetic Resonance (2020) 51:1071–1078
https://doi.org/10.1007/s00723-020-01258-2

Applied
Magnetic Resonance

ORIGINAL PAPER

Charge photogeneration and Recombination in Ternary Organic Photovoltaic Blend PCDTBT/PC60BM/ICBA Studied by EPR Spectroscopy

Leonid V. Kulik[1,2] · **Mikhail N. Uvarov**[1,2]

Received: 2 July 2020 / Revised: 14 August 2020 / Published online: 3 September 2020

Abstract

Using the stationary and pulsed EPR methods, the ternary composite PCDTBT and two fullerene acceptors PCDTBT/PC_{60}BM/ICBA 1:1:1, as well as the corresponding binary composites PCDTBT/PC_{60}BM 1:2 and PCDTBT/ICBA 1:2, were studied at a temperature of 80 K. Modeling these spectra allows us to estimate the contributions of PC_{60}BM and ICBA to the light-induced EPR signal of the PCDTBT/PC_{60}BM/ICBA ternary composite as 0.7:0.3. The absence of new lines in the EPR spectrum of the ternary composite, in comparison with the corresponding binary ones, means that the mechanism of the molecular alloy of PC_{60}BM and ICBA, as previously assumed, is not operative in this system, and the most probable scenario is the existence of two parallel heterojunctions PCDTBT/PC_{60}BM and PCDTBT/ICBA. This conclusion is confirmed by modeling the decay curves of the light-induced EPR upon turning off the light, as well as the out-of-phase electron spin echo from the charge transfer state (the main intermediate of the photoelectric conversion) in these composites. It is noteworthy that in the ternary composite with the same fullerene acceptors, but with a different polymer donor (P3HT), the molecular alloy mechanism of two acceptors is realized (Angmo et al. in J Mater Chem C 3: 5541–5548, 2015). It is likely that the polymer donor has a decisive influence on the morphology and electron-transport properties of such ternary composites. It should be noted that the methods of light-induced EPR and out-of-phase ESE were used for the first time to study ternary donor–acceptor composites.

✉ Leonid V. Kulik
chemphy@kinetics.nsc.ru

[1] Voevodsky Institute of Chemical Kinetics and Combustion SB RAS, Institutskaya Str. 3, 630090 Novosibirsk, Russia

[2] Novosibirsk State University, Pirogova Str. 2, 630090 Novosibirsk, Russia

1 Introduction

Organic photovoltaics is promising and fast-developing field of solar technology. Even active layer of several hundred nanometers thickness can absorb substantial part of solar light of visible spectrum, giving an opportunity to make flexible and space-saving organic solar cells. Unlike inorganic devices, mostly silicon made, production of organic cells is expected to be cheap and environmentally friendly. Conventional architecture imposes using two-component donor–acceptor composites as active layer of a cell. Nevertheless, it limits a cell's feasible efficiency mostly due to solar light being consumed in a rather narrow spectral band. One can use more complex architectures, like ternary junction cells, to overcome this limitation. Active medium of ternary cells consists of three different organic compounds. Some of such devices based upon conjugated polymers and fullerene derivative or non-fullerene molecules have been already tested by several research groups. Even though numerous ternary systems reveal high efficiency factor up to 17% [1], the photovoltaic conversion mechanism behind them is not understood that well as for binary systems. Complexity of ternary donor–acceptor composites demands a variety of experimental techniques to be used for elucidating the mechanism of photoelectric conversion. Since most of the intermediates of photoelectric conversion are paramagnetic [2–9], EPR is a method of choice for studying its mechanism. Here, we tested the applicability of CW and pulse EPR methods, including out-of-phase electron spin echo (ESE) spectroscopy [9, 11, 12], previously used only for binary donor–acceptor composites.

2 Experimental Section

The chlorobenzene solutions of PCDTBT (Poly[*N*-9′-heptadecanyl-2,7-carbazole-alt-5,5-(4′,7′-di-2-thienyl-2′,1′,3′-benzothiadiazole)], Ossila) and $PC_{60}BM$ ([6,6]-Phenyl-C61-butyric acid methyl ester, Ossila) and/or ICBA (1′,1′′,4′,4′′-tetrahydro-di[1,4]methanonaphthaleno[5,6]fullerene-C60, Ossila) with the proper weight of the solutes were prepared with total concentration of 30 mg/ml. The solutions were put in the EPR tube of 4.8 mm outer diameter, and three freeze-pump-thaw cycles were performed. Chlorobenzene was evaporated in the vacuum of about 0.1 torr, which resulted in the formation of the polymer/fullerene composite on the inner wall of the EPR sample tube. For all samples the weight ratio of donor PCDTBT and acceptor ($PC_{60}BM$, ICBA or their mixture) was 1:2, which corresponds to optimal ratio for PCDTBT/ $PC_{60}BM$ photovoltaic devices [13].

CW EPR and ESE measurements were carried out on an X-band ELEXSYS ESP-580E EPR spectrometer equipped with an ER 4118 X-MD-5 dielectric cavity inside an Oxford Instruments CF 935 cryostat. Temperature was kept at 80 K by cold nitrogen gas flow.

To measure the light-induced EPR (LEPR) signal, the samples inside EPR resonator were irradiated by actinic lamp (incident light power density 200 mW/cm^2).

ESE inversion-recovery dependencies were measured using $\pi - T - \pi/2 - \tau - \pi$ pulse sequence under continuous light illumination. The mw pulse amplitude was sufficiently low to excite only the EPR line of $PCDTBT^+$ hole or electron at fullerene acceptor. The duration of π-pulse was 200 ns.

Laser flashes from TECH-laser (Laser-export Co. Ltd., Russia) with wave length 527 nm, pulse duration of about 5 ns, and pulse repetition rate of 1 kHz illuminated the sample in out-of-phase ESE experiments. The laser light was directed to the refractive lens along its optical axis and gone inside the EPR tube through quartz light guide. The energy of the flash was about 15 μJ reached the sample.

ESE signal was obtained using a two-pulse mw pulse sequence applied after a laser flash, Flash – DAF – $\pi/4$ – τ – π-echo, where *DAF* is the Delay After laser Flash (200 ns), the $\pi/4$- and π-pulses were of 8 ns and 24 ns nominal duration, respectively, the initial τ delay was 160 ns. As we noted previously [11], real duration of mw pulses is slightly shorter than their nominal duration in our pulse EPR setup. For this reason mw pulses of 8 ns and 24 ns nominal duration with equal amplitude corresponds approximately to $\pi/4$ and π magnetization turning angles, respectively. The phase for the ESE was adjusted to obtain zero out-of-phase ESE signal at DAF = 990 μs. The pre-saturating $\pi/2$-pulse was applied to cancel ESE signal of the long-living species and to measure the out-of-phase ESE signals of CTS. The delay between the pre-saturating $\pi/2$-pulse with 20 ns duration and laser flash was 2 μs and this mw pulse affected only the photoaccumulated paramagnetic species (electrons and holes in deep traps). The magnetic field B_0 corresponded to the deep between the EPR lines of $PCDTBT^+$ and fullerene acceptor, to ensure nearly homogeneous mw excitation of the EPR spectrum. Overall, the experimental conditions were similar to those in our recent out-of-phase ESE study [14].

3 Results and Discussion

3.1 Light-Induced EPR and Magnetization Inversion-Recovery

Initially, to assign the signals of photogenerated paramagnetic species in the composites, light-induced EPR spectra were recorded. As expected, all the composites studied (PCDTBT/$PC_{60}BM$, PCDTBT/ICBA and PCDTBT/$PC_{60}BM$/ICBA) demonstrated weak dark EPR signal and strong light EPR signal, which is typical for efficient organic photovoltaic blends [15–17]. The spectra are compared at Fig. 1. For all the composites the identical broad line at low field is observed which is readily assigned to $PCDTBT^+$; its g value is close to free-electron g value [18]. The sharp intense line at higher field for PCDTBT/$PC_{60}BM$ composite is evidently assigned to $PC_{60}BM^-$. For PCDTBT/ICBA composite the high-field line has similar shape but much lower intensity. It is assigned to $ICBA^-$. Low g factors for anion-radicals of C_{60}-based molecules $PC_{60}BM$ and ICBA are caused by Jahn–Teller effect in fullerene moiety [19]. As will be shown below, the dramatic decrease of the intensity of $ICBA^-$ line is caused by mw power saturation due to its very long spin–lattice relaxation time T_1. The difference of the relaxation properties allows to distinguish EPR signals of $PC_{60}BM^-$ and $ICBA^-$, despite their very close g factors and linewidth.

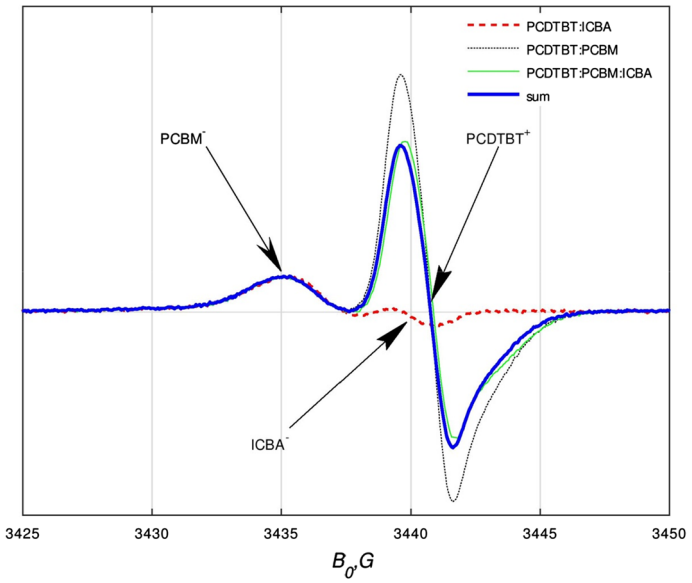

Fig. 1 Light-induced EPR spectra for PCDTBT/$PC_{60}BM$ 1:2 composite (black dotted line), PCDTBT/ICBA 1:2 composite (red dashed line), and PCDTBT/$PC_{60}BM$/ICBA 1:1:1 composite (thin green line). Weighted average (0.7:0.3) of the spectra for PCDTBT/$PC_{60}BM$ and PCDTBT/ICBA thick blue line. Temperature 80K, microwave power 0.2 mW, modulation amplitude 1 G. The arrows mark spectral positions at which inversion-recovery experiments (Fig. 2) were performed (color figure online)

This allows us to estimate the contributions of $PC_{60}BM^-$ and $ICBA^-$ to the light-induced EPR signal of the PCDTBT/$PC_{60}BM$/ICBA ternary composite as 0.7:0.3, since the spectrum of the ternary composite is well approximated by the sum of the spectra of the corresponding binary composites with the corresponding weights. The absence of new lines in the EPR spectrum of the ternary composite, in comparison with the corresponding binary ones, means that the mechanism of the molecular alloy $PC_{60}BM$ and ICBA previously assumed in Ref. [20] is not realized in the system under the study, and the most probable scenario is the existence of two parallel heterojunctions PCDTBT/$PC_{60}BM$ and PCDTBT/ICBA. The smaller contribution of ICBA to charge separation with the same $PC_{60}BM$ and ICBA content in the composite indicates a more efficient charge transfer in the PCDTBT/$PC_{60}BM$ transition.

The relaxation properties of light-induced species in these composites were investigated by the inversion-recovery method in pulsed EPR. The inversion-recovery curves at 80 K are well approximated by the Kohlrausch function (stretched exponential, $f = A \times \exp[-(T/T_1)^b]$), see Fig. 2. Some difference from the monoexponential recovery of magnetization is explained by the T_1 value distribution, which is typical for disordered heterojunctions. Despite some difference in the exponent b, the characteristic values of T_1 at 80 K for the $PCDTBT^+$ hole and $ICBA^-$ electron are close and exceed significantly the value for $PC_{60}BM^-$ (see Table 1). The difference in the spectra of the light-induced EPR of the composites PCDTBT/$PC_{60}BM$ and PCDTBT/ICBA is caused by the saturation of the

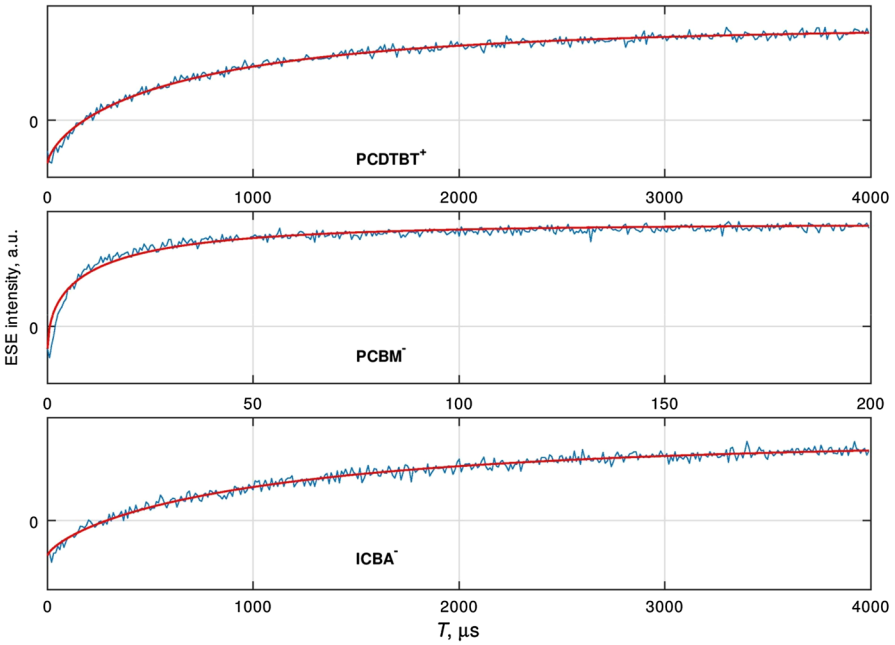

Fig. 2 Light-induced signal inversion-recovery curves in the PCDTBT/PC60BM composite for the $PCDTBT^+$ hole (upper panel) and $PC60BM^-$ electron (middle panel). The same for the $ICBA^-$ electron in the PCDTBT/ICBA composite (bottom panel). Temperature 80 K. Red lines approximation of inversion-recovery curves by the Kohlrausch function (color figure online)

Table 1 The parameters of numerical simulations of ESE inversion-recovery traces (Fig. 2) by the stretched exponential functions $f \sim \exp(-T/T_1)^b$

Species	T_1 (µs)	b
$PCDTBT^+$	730	0.7
$PC_{60}BM^-$	11	0.53
$ICBA^-$	1120	0.74

EPR signal of $ICBA^-$ at 80 K. Due to the fast spin-lattice relaxation, $PC_{60}BM^-$ avoids saturation and provides large contribution to light-induced EPR signal.

The decay curves of the light-induced EPR on the $PCDTBT^+$ signal were detected when the light was turned off (see Fig. 3). All other conditions were the same as for light-induced EPR spectra measurement. These curves differ markedly for the three composites PCDTBT/PC_{60}BM, PCDTBT/ICBA and PCDTBT/PC_{60}BM/ICBA. The depth of the initial rapid decline (the first few tens of seconds) for the PCDTBT/PC_{60}BM composite is much less than for the PCDTBT/ICBA. This indicates larger effective charge mobility in the PCDTBT/PC_{60}BM composite. The EPR signal decay kinetics for the PCDTBT/PC_{60}BM/ICBA ternary composite has an intermediate initial decay depth and is again well approximated by the sum of the kinetics for the PCDTBT/PC_{60}BM and PCDTBT/ICBA

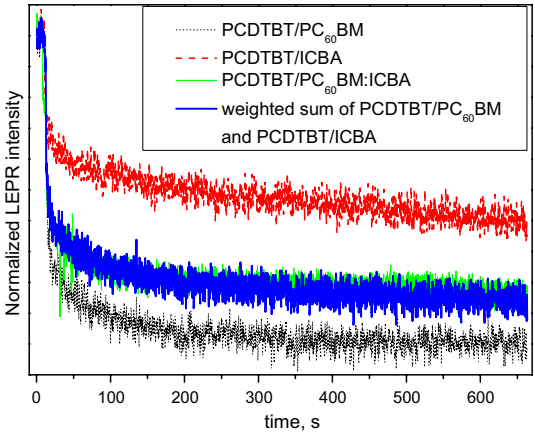

Fig. 3 Normalized decay kinetics of a light-induced EPR signal in composites PCDTBT/$PC_{60}BM$ 1:2 (black dotted line), PCDTBT/ICBA 1:2 (red dashed line), and PCDTBT/$PC_{60}BM$/ICBA 1:1:1 (thin green line). Weighted average (0.7:0.3) of the decay kinetics for PCDTBT/$PC_{60}BM$ and PCDTBT/ICBA thick blue line. Temperature 80K, microwave power 0.2 mW, modulation amplitude 1 G (color figure online)

composites in weights of 0.7: 0.3, which is further confirmation of the parallel heterojunction scenario.

3.2 Out-of-Phase ESEEM

The charge transfer state for these composites was studied by the out-of-phase electron spin echo method in a two-pulse experiment. This method was developed while investigating light-induced photosynthetic electron transfer [21]. It was realized that appearance of this signal is a signature of electron spin correlation within photogenerated radical pair [22–24]. The dependencies of the out-of-phase ESE signal on the interval between microwave pulses are significantly different for PCDTBT/$PC_{60}BM$ and PCDTBT/ICBA composites, see Fig. 4. In the latter case, the out-of-phase ESE signal has the highest modulus (negative) intensity for τ interval of 300 ns, and for 700 ns in the first case. The faster evolution of the out-of-phase ESE signal in PCDTBT/ICBA indicates a greater magnitude of the magnetic interaction between the electron and the hole within the charge transfer state than for PCDTBT/$PC_{60}BM$. The greater charge transfer distance during thermalization in PCDTBT/$PC_{60}BM$ composite is the likely cause of a more efficient charge separation in this heterojunction than in PCDTBT/ICBA composite. Similar to the previous cases, the out-of-phase ESE signal in the PCDTBT/$PC_{60}BM$/ICBA composite is well approximated by the weighted sum of the signals from the corresponding binary composites, which fits into the model of parallel heterojunctions. This implies the existence of two different CTSs at donor/acceptor interfaces of the ternary composite, which both are spin-correlated radical pairs. However, the signal-to-noise ratio does not allow us to accurately determine the relative contributions of these transitions to the formation of the with charge transfer state, which can be both 0.7:0.3 (as in the cases considered above) and 0.5:0.5. Overall, CTS dynamics in the ternary composite PCDTBT/$PC_{60}BM$/ICBA is in accordance with the model of two parallel heterojunctions. It is likely that CTSs in a ternary composite are generated with the same efficiency at two parallel heterojunctions, but geminate recombination more strongly

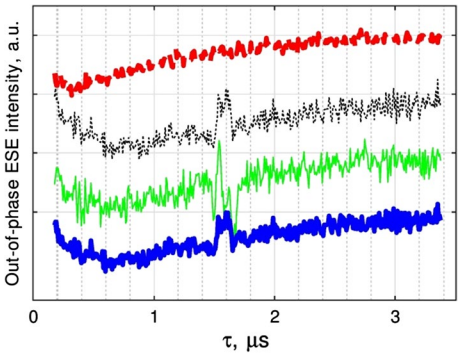

Fig. 4 The dependence of the out-of-phase ESE signal on the delay between microwave pulses in composites PCDTBT/$PC_{60}BM$ 1:2 (black dotted line), PCDTBT/ICBA 1:2 (red dashed line), and PCDTBT/$PC_{60}BM$/ICBA 1:1:1 (thin green line). Weighted average (0.7:0.3) of the decay kinetics for PCDTBT/$PC_{60}BM$ and PCDTBT/ICBA thick blue line. DAF = 200 ns. Temperature 80 K. The curves are spaced apart in height; they approach zero level for long τ delays. The feature at $\tau = 1.6$ μs is caused by an undesired echo from the pre-saturation pulse and the $\pi/4$ pulse, which creates out-of-phase ESE (color figure online)

reduces the yield of free charges in the PCDTBT/ICBA transition due to the shorter initial charges separation distance. This explains the predominance of the $PC_{60}BM^-$ signal over $ICBA^-$ in the spectrum of stationary light-induced EPR, since it is exclusively the separated charges that contribute to this spectrum. It is noteworthy that in a ternary composite with the same fullerene acceptors, but with a different polymer donor (P3HT), the molecular alloy mechanism of two acceptors is realized [20]. For molecular alloy, the averaging of the properties of two acceptors is expected [25]. The polymer donor probably has a decisive influence on the morphology and electron-transport properties of such ternary composites.

4 Conclusions

For the first time methods of light-induced EPR and out-of-phase ESE are used to study ternary donor–acceptor organic photovoltaic composite. For the composite of conjugated polymer PCDTBT and two fullerene acceptors $PC_{60}BM$ and ICBA the difference of spin–lattice relaxation rate of photogenerated electrons $PC_{60}BM^-$ and $ICBA^-$ allows to distinguish their contributions to light-induced EPR spectra, despite quite similar g factors and linewidth. The set of data, including light-induced EPR spectra, light-induced EPR decay curves and two-pulse out-of-phase ESE traces for ternary PCDTBT/$PC_{60}BM$/ICBA composite can be reasonably approximated by the weighted average of the corresponding data for binary composites PCDTBT/$PC_{60}BM$ and PCDTBT/ICBA with the same weight proportion 0.7:0.3. This is a strong argument for existence of two parallel donor/acceptor heterojunctions in this composite, rather than molecular alloy scenario often suggested for composites with two fullerene acceptors.

Acknowledgments This work was supported by Russian Foundation for Basic Research, grant 19-03-00149.

References

1. X. Du, Y. Yuan, L. Zhou, H. Lin, C. Zheng, J. Luo, Z. Chen, S. Tao, L.-S. Liao, Adv. Funct. Mater. **30**, 1909837 (2020)
2. L. Pasimeni, L. Franco, M. Ruzzi, A. Mucci, L. Schenetti, C. Luo, D.M. Guldi, K. Kordatos, M. Prato, J. Mater. Chem. **11**, 981 (2001)
3. C. Deibel, T. Strobel, V. Dyakonov, Adv. Mater. **22**, 4097 (2010)
4. J. Niklas, S. Beaupré, M. Leclerc, T. Xu, L. Yu, A. Sperlich, V. Dyakonov, O.G. Poluektov, J. Phys. Chem. B **119**, 7407 (2015)
5. A. Konkin, A. Popov, U. Ritter, S. Orlinskii, G. Mamin, A. Aganov, A.A. Konkin, P. Scharff, J. Phys. Chem. C **120**, 28905 (2016)
6. F. Kraffert, J. Behrends, Mol. Phys. **115**, 2373 (2017)
7. E.A. Lukina, E. Suturina, E. Reijerse, W. Lubitz, L.V. Kulik, Phys. Chem. Chem. Phys. **19**, 22141 (2017)
8. Y. Hou, X. Zhang, K. Chen, D. Liu, Z. Wang, Q. Liu, J. Zhao, A. Barbon, J. Mater. Chem. **7**, 12048 (2019)
9. E.A. Lukina, E. Reijerse, W. Lubitz, L.V. Kulik, Mol. Phys. **117**, 2654 (2019)
10. E.A. Lukina, A.A. Popov, M.N. Uvarov, L.V. Kulik, J. Phys. Chem. B **119**, 13543 (2015)
11. E.A. Lukina, A.A. Popov, M.N. Uvarov, E.A. Suturina, E.J. Reijerse, L.V. Kulik, Phys. Chem. Chem. Phys. **18**, 28585 (2016)
12. M.N. Uvarov, L.V. Kulik, Appl. Magn. Reson. **50**, 1277 (2019)
13. S. Wakim, S. Beaupre, N. Blouin, B.-R. Aich, S. Rodman, R. Gaudiana, Y. Tao, M. Leclerc, J. Mater. Chem. **19**, 5351 (2009)
14. E.A. Beletskaya, E.A. Lukina, M.N. Uvarov, A.A. Popov, L.V. Kulik, J. Chem. Phys. **152**, 044706 (2020)
15. V. Dyakonov, G. Zoriniants, M. Scharber, C.J. Brabec, R.A.J. Janssen, J.C. Hummelen, N.S. Sariciftci, Phys. Rev. B **59**, 8019 (1999)
16. H. Tanama, N. Hasegawa, T. Sakamoto, K. Marumoto, S.-I. Kuroda, Jpn. J. Appl. Phys. **46**, 5187 (2007)
17. E.A. Lukina, M.N. Uvarov, L.V. Kulik, J. Phys. Chem. C **118**, 18307 (2014)
18. J. Niklas, K.L. Mardis, B.P. Banks, G.M. Grooms, A. Sperlich, V. Dyakonov, S. Beaupre, M. Leclerc, T. Xu, L. Yu, O.G. Poluektov, Phys. Chem. Chem. Phys. **15**, 956 (2013)
19. J. De Ceuster, E. Goovaerts, A. Bouwen, J.C. Hummelen, V. Dyakonov, Phys. Rev. B **64**, 195206 (2001)
20. D. Angmo, M. Bjerring, N.C. Nielsen, B.C. Thompson, F.C. Krebs, J. Mater. Chem. C **3**, 5541 (2015)
21. S.A. Dzuba, P. Gast, A.J. Hoff, Chem. Phys. Lett. **236**, 595 (1995)
22. K.M. Salikhov, YuE Kandrashkin, A.K. Salikhov, Appl. Magn. Reson. **3**, 199 (1992)
23. J. Tang, M.C. Thurnauer, A. Kubo, H. Hara, A. Kawamori, J. Chem. Phys. **106**, 7471 (1997)
24. A.J. Hoff, P. Gast, S.A. Dzuba, C.R. Timmel, C.E. Fursman, P.J. Hore, Spectrochim. Acta A **54**, 2283 (1998)
25. L. Lu, M.A. Kelly, W. You, L. Yu, Nat. Photonics **9**, 491 (2015)